

# Transient Approximation of SAFE-100 Heat Pipe Operation

Shannon M. Bragg-Sitton and Robert S. Reid

*NASA Marshall Space Flight Center, Propulsion Research Center, Huntsville, AL 35758*  
*Los Alamos National Laboratory, Los Alamos, NM 87545*  
*256-544-6272; [Shannon.bragg-sitton@msfc.nasa.gov](mailto:Shannon.bragg-sitton@msfc.nasa.gov)*

**Abstract.** Engineers at Los Alamos National Laboratory (LANL) have designed several heat pipe cooled reactor concepts, ranging in power from 15 kWt to 800 kWt, for both surface power systems and nuclear electric propulsion systems. The Safe, Affordable Fission Engine (SAFE) is now being developed in a collaborative effort between LANL and NASA Marshall Space Flight Center (NASA/MSFC). NASA is responsible for fabrication and testing of non-nuclear, electrically heated modules in the Early Flight Fission Test Facility (EFF-TF) at MSFC. In-core heat pipes must be properly thawed as the reactor power starts. Computational models have been developed to assess the expected operation of a specific heat pipe design during start-up, steady state operation, and shutdown. While computationally intensive codes provide complete, detailed analyses of heat pipe thaw, a relatively simple, concise routine can also be applied to approximate the response of a heat pipe to changes in the evaporator heat transfer rate during start-up and power transients (e.g., modification of reactor power level) with reasonably accurate results. This paper describes a simplified model of heat pipe start-up that extends previous work and compares the results to experimental measurements for a SAFE-100 type heat pipe design.

## INTRODUCTION: THEORY OF HEAT PIPE OPERATION

A heat pipe is a closed, passive heat transfer device that is generally constructed from a long cylindrical pipe that is sealed at both ends and is partially filled with a working fluid. Heat pipes are self-starting, and they have a self-pumping coolant loop; pumping action is accomplished by a porous wick structure along the inside surface of the heat pipe. A discussion of the theory of heat pipe operation can be found in (Faghri, 1995).

In a heat pipe with a crescent annular wick structure, working fluid is held within a gap between the wick and the wall, leaving a void in the central region. A heat pipe consists of three distinct regions along the axial dimension: the evaporator, which is actively heated; the adiabatic region, which is neither heated nor cooled; and the condenser, which is actively cooled. Although the evaporator and condenser regions are required, not all heat pipes are operated with an adiabatic region, depending on the specific application. When the evaporator region is heated, the liquid metal begins to boil and is vaporized. In an alkali metal heat pipe, the working fluid is generally evaporated by surface vaporization that occurs at the liquid-vapor interface. The vapor escapes the porous wick structure and diffuses into the central void. The pressure differential along the heat pipe moves vapor along the central column toward the cooler, lower pressure condenser region. The lower temperature in this region causes the vapor to condense on the wick surface, liberating latent heat of vaporization. This heat is transferred through the heat pipe wall to the external environment. Coupling the heat pipe to a heat exchanger can capture this energy. The condensate is again held by the wick and is pumped by capillary action in the wick structure back to the evaporator region, where it can again be vaporized. An illustration of the vapor and liquid flow in an operating heat pipe is shown in Figure 1. This process establishes a closed loop system in which heat is removed from the heated evaporator region and is transferred to the environment around the condenser. The condenser region is generally coupled to a heat exchanger for energy conversion.

Several features demonstrated by heat pipes are desirable in space systems, and they are often considered for reactor cooling and waste heat rejection in radiator panels. Heat pipes are capable of transferring large amounts of energy over a wide range of temperatures, where the desired operating temperature and power throughput are used to select an appropriate heat pipe design. Passive heat pipe operation removes additional system complexities that are

introduced in many heat transfer designs, such as active cooling to a reactor core utilizing high-pressure gas flow or a pumped liquid metal loop. Additionally, because each heat pipe is independent, a heat pipe cooled system is a redundant design (e.g., 127 core heat pipes in the SAFE-400 design (Poston, 2002)), increasing failure tolerance by removing single point failure mechanisms. Experimental operation of a sodium filled stainless steel heat pipe, designed for electrically heated testing of the SAFE-100a reactor core prototype, is discussed in this paper.

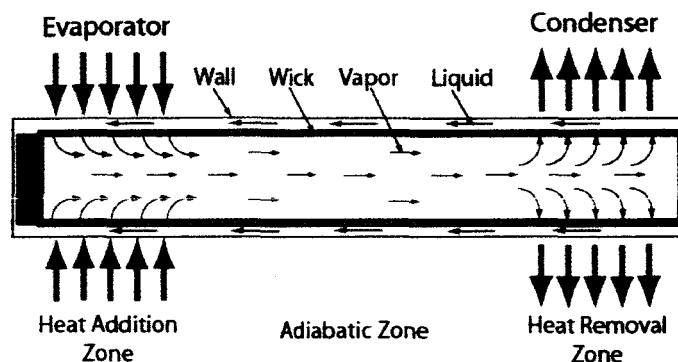


FIGURE 1. Illustration of Heat Pipe Operation.

The selection of an appropriate working fluid is dependent on the desired heat pipe operating temperature (Hall and Doster, 1990). For high temperature applications, above 700 K, alkali metal heat pipes are an appropriate choice. Sodium and lithium heat pipes, for instance, can provide power throughputs as high as 15 and 30 kW/cm<sup>2</sup> at operating temperatures of 1150 and 1580 K, respectively (Tournier and El-Genk, 2003).

For a heat pipe to operate properly, the maximum capillary pressure rise, which is determined by the effective pore radius in the wick, must exceed the total pressure drop in the liquid and vapor regions. The liquid pressure drop in the heat pipe wick is purely viscous, but the vapor pressure drop in the evaporator and condenser regions is more complicated due to the presence of both viscous and inertial effects. Details of the pressure drop in each region are provided in Reid (2003).

Heat pipes are filled to a specified mass of high purity alkali metal by vacuum distillation (Martin and Salvail, 2004). During heat pipe fill, a plug at the evaporator end seals off the tube. The condenser end is sealed by "excess" working fluid; this corresponds to approximately 10% greater than what is required to saturate the wick, forming a "pool" at the end of the condenser. After the fill is complete, the heat pipe fill stem is crimped and welded to seal off the heat pipe. Before using a heat pipe, it must be heated isothermally along the entire length to ensure that the entire wick has been wetted by the alkali metal working fluid (e.g., Na) before use as a heat transfer mechanism.

### Transient Heat Pipe Operation

Depending on the stage of operation of a heat pipe, various restrictions limit the rate at which it can transfer heat. During heat pipe start-up, heat input in the evaporator region begins to melt the working fluid that is trapped in the wick. The vapor flow moves through several flow regimes during start-up, including molecular flow, transition flow, and continuum or viscous flow. At the melt front that propagates toward the condenser end, all three flow regimes may coexist (Tournier, 2003). Once the continuum flow reaches the end of the condenser, a liquid plug forms and the heat pipe becomes operational. Little working fluid mass is lost to the vapor flow by sublimation, such that the evaporator wick remains saturated with liquid throughout a proper start-up.

During start-up or low power operations, a heat pipe is viscous limited. During this period, the low vapor pressure is insufficient to overcome the pressure drop along the full length of the pipe and the vapor cannot travel the full length of the condenser, effectively shortening the active length of the heat pipe. At slightly higher power density, but still during heat pipe start-up, the heat pipe can become sonic limited. During this period, the vapor is traveling at high velocity through the evaporator region, but it cannot exceed sonic velocity at the evaporator exit. If the vapor reaches the speed of sound, choking occurs at the evaporator exit (Tournier, 2003). The sonic limit for energy

transfer rate along the heat pipe ( $\dot{Q}_{sonic}^{limit}$ ) is expressed in Eq. (1), where  $\dot{Q}$  is the actual energy transfer rate from the evaporator to the condenser region. All variables are defined in the *Nomenclature* section at the end of this paper.

$$\dot{Q} \leq \dot{Q}_{sonic}^{limit} = 0.474 h_{fg} A_v (2.08 p_0 \rho_0)^{1/2} \quad (1)$$

While the heat pipe is sonic limited, further heat input causes the evaporator region to heat up relative to the condenser region. If a heat pipe is started very slowly, it does not reach the sonic limit. The nominal start-up time varies depending on the heat pipe design.

The minimum of the radiation, sonic, and viscous heat transfer limits provides an estimate of the heat transfer rate from the evaporator to the condenser during heat pipe start-up (Reid, 2002). The radiation heat transfer limit ( $\dot{Q}_R$ ), given by Eq. (2), represents the maximum amount of heat that can be transferred from the evaporator to the condenser, and subsequently to the environment. The radiation heat transfer limit assumes that *all* the heat from the evaporator is fully transferred to the condenser, which is then radiated to the environment:

$$\dot{Q}_R = \sigma \epsilon A_{Cond} (T_{Evap}^4 - T_{\infty}^4) \quad (2)$$

The viscous limit ( $\dot{Q}_V$ ) is determined by the point at which the total pressure drop along the heat pipe is equal to the saturation pressure at the evaporator outlet temperature. The total pressure drop is the sum of the vapor pressure drop in the evaporator and condenser and the liquid pressure drop experienced by the working fluid as it travels through the wick from the condenser back to the evaporator. During heat pipe operation, a capillary limit is also present at a power level that produces a mass flow rate of the working fluid sufficient for the liquid and vapor pressure drops to exceed the maximum capillary head potential in the wick. During this stage, the mass of vapor leaving the evaporator region exceeds the mass of liquid returning along the wick. This results in a rising evaporator temperature due to liquid depletion (i.e. the evaporator cooling is reduced due to a smaller amount of liquid returning from the condenser region).

## HEAT PIPE OPERATION: EXPERIMENTAL AND COMPUTATIONAL ANALYSES

For nominal operation of a heat pipe reactor, the in-core heat pipes must be properly thawed as the reactor power is slowly increased. A slow start-up prevents potentially problematic events such as entrainment, departure from nucleate boiling in the evaporator region, or evaporator dryout. Computational models have been developed to assess the expected operation of a specific heat pipe design both during start-up and steady state operation. Some codes provide complete, detailed analyses of heat pipe thaw that are computationally intensive (Cao and Faghri 1992; Hall and Doster 1990; Tournier and El-Genk 1995; Tournier and El-Genk 1996; Tournier and El-Genk 2003; Tournier and El-Genk 1993). A relatively simple, concise routine can also be applied to approximate the response of a heat pipe to changes in the evaporator heat transfer rate during start-up and power transients (e.g., modification of reactor power level) with reasonably accurate results (Reid, 2002; Reid et al., 2001). In this paper a simplified model of heat pipe start-up is developed by extending the work of Reid (2002), and comparing the results to experimental measurements for a SAFE-100 type heat pipe design.

Heat pipe start-up and restart (freeze-thaw) has been well characterized experimentally and summarized in the literature. Heat pipe frozen start-up and restart physics have been closely examined in numerous computational models. Since September 2000, SAFE-30 and SAFE-100 heat pipes at NASA MSFC and JPL have undergone hundreds of restarts without a single problem. Reliability of this sort is the norm for properly designed and integrated alkali metal heat pipes.

Reactor thermal transients are typically slow compared with the response potential of fixed conductance core heat pipes. So long as condenser heat rejection loads are kept within reasonable bounds at low temperature, initial core start-up and restarts should be smooth and trouble-free. Heat pipe component tests permit system freeze-thaw to be characterized early in system design process.

## Transient Operation of a Sodium Heat Pipe

Computational analysis of heat pipe start-up requires a detailed description of the module geometry and boundary conditions. In preparation for the SAFE-100a tests, each heat pipe module underwent multiple start-ups as the final stage in the standard heat pipe processing procedures, which included fill, leak check, vacuum processing, weld closeout, and high temperature "wet-in" (Martin and Salvail, 2004). The data presented in this paper for comparison to computational results correspond to the second start-up of SAFE-100a Module 12 that was performed at the EFF-TF facility in October 2003. The heat pipe was operated in air, with heating provided by three cartridge heaters (boroelectric heater elements, Advanced Ceramics Corporation) that fit into the three fuel tubes surrounding the central heat pipe in the module. Due to the limited length of the heater elements, the evaporator region was effectively limited to 40.6 cm (16 in). This configuration is illustrated in Figure 2.

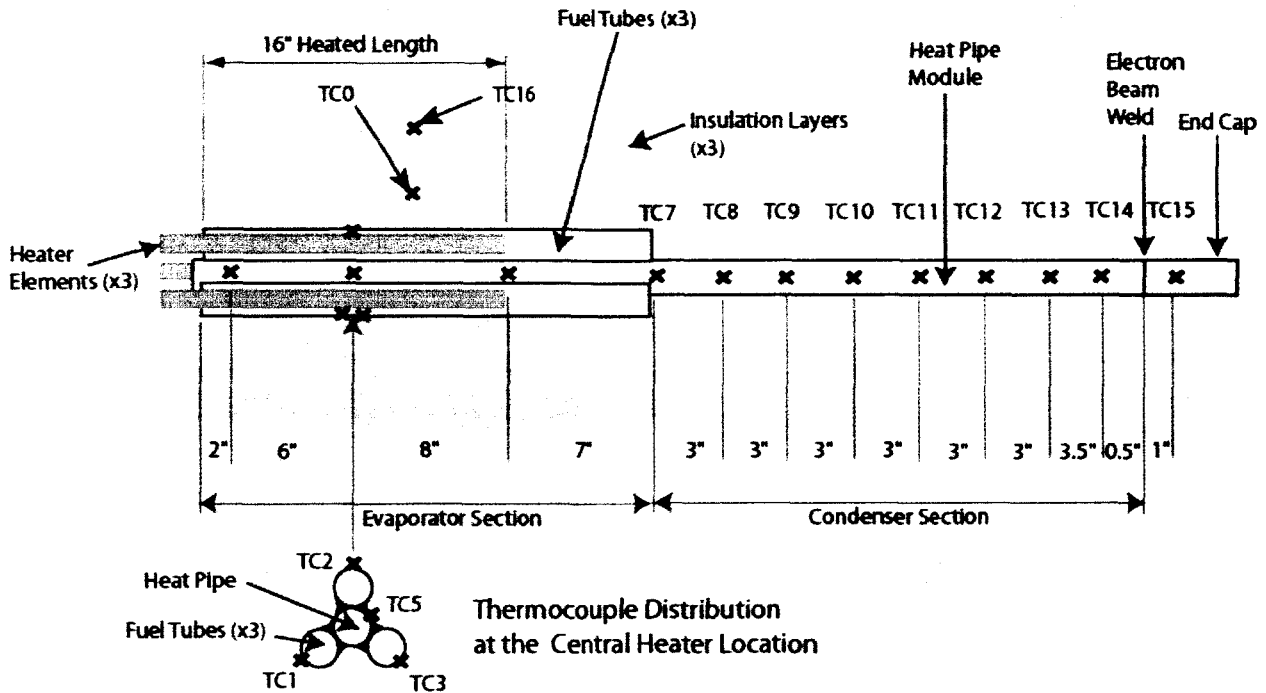


FIGURE 2. General Component Layout for Heat Pipe Testing with TC Locations.

To monitor the start-up process, the module was instrumented with 15 type K thermocouples (TCs) that were distributed along its length and spot-welded to the desired tube surface. Thermocouples were placed such that 3 were located on the external surfaces of the fuel tubes, 3 were located on the evaporator section, 8 were located on the condenser section, and one was located on the end cap. An "x" in Figure 2 notes the location of each thermocouple.

For module testing, the fuel tubes and evaporator section were wrapped with three layers of 1" thick insulation material (Insulfrax) with an outer layer of foil to decrease the thermal losses to the environment. The evaporator insulation was equipped with two thermocouples to provide an estimate of the ambient losses. Heat pipe start-up was performed over approximately one hour to an average condenser temperature of 930 K (660°C), which was maintained for approximately 6 hours. During testing, the heat pipe condenser section was also loosely covered with a single layer of aluminum foil.

## Computational Heat Pipe Analysis

A relatively simple approach was taken in developing a computational model of heat pipe operation during start-up. Computational analysis of a SAFE-100a heat pipe was based on the transient heat pipe response approximation, HPAPPX, that was developed by Reid (2002) for the SAFE-30 heat pipe design (Reid et al., 2001). The original HPAPPX code, written in Fortran, made several simplifying assumptions to minimize the computation time, yet maintain reasonably accurate results. The approach first assumed that the alkali metal heat pipe maintained a fixed conductance, and that changes in the evaporator heat transfer rate were quasi-steady. In this one-dimensional approach to heat pipe start-up and operation, a lumped capacitance solution was applied. Additional assumptions included viscous limited, laminar, and incompressible flow. The modeled heat pipe was not sonic limited during start-up, so this limitation to the heat transfer rate was not included. Although HPAPPX provides a reasonable approximation to heat pipe transients, it was not designed to predict the transient response in a rapid heat pipe start-up from a frozen state.

Several modifications were required to apply HPAPPX to the SAFE-100a geometry. In the earlier SAFE-30 design, each individual module was constructed from a central heat pipe with one half of its circumference ( $\pi$  radians) surrounded by four fuel tubes (see Fig. 3a), providing significantly improved coupling between the heat pipe and fuel tubes (cartridge heaters) than in the tri-node SAFE-100 design (see Fig. 3b,c). Additionally, SAFE-30 module testing was performed in vacuum, such that no heat was lost due to convective heat transfer, and the heated region was not surrounded by insulation, such that heat loss from the fuel tubes and the evaporator region was possible by radiation.

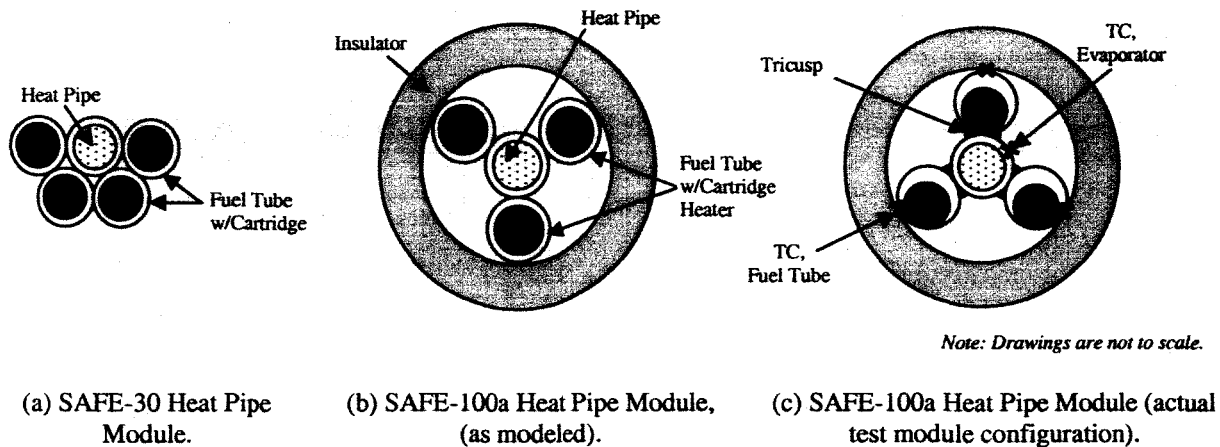


**FIGURE 3.** Heat Pipe Modules Modeled by HPAPPX.

The cartridge heater (CH) and fuel tube (FT) configuration was modeled as a simple two-zone enclosure with series resistances. Although the cartridge heaters were slid into the fuel tubes and simply allowed to rest in the tube, the model assumed that the heaters were centered in the fuel tubes (not touching the walls). Hence, it was assumed that conduction between the heater, fuel tube was minimal, and only radiation heat transfer from the heater to the tube wall was included. Applying these assumptions, the expression for the heat transfer from the heater (CH) to the fuel tube (FT) was determined using Eqs. (3), where  $\epsilon$ ,  $A$ , and  $T$  correspond to the emittance (unitless), area ( $m^2$ ), and temperature (K) of each component. The energy at each node is given by  $\sigma T^4$ , where  $\sigma$  is the Stefan-Boltzmann constant ( $5.67 \times 10^{-8} \text{ W/m}^2 \cdot \text{K}^4$ ).

$$Q_{CH} = \frac{\sigma(T_{CH}^4 - T_{FT}^4)}{R} = G_{RI}(T_{CH}^4 - T_{FT}^4) \quad (3a)$$

$$R = \frac{1}{A_{CH}} \left( \frac{1}{\epsilon_{CH}} + \frac{A_{CH}}{A_{FT}} \left( \frac{1}{\epsilon_{FT}} - 1 \right) \right) \quad (3b)$$

Note that in the derivation of the equivalent resistance between the cartridge heater and the fuel tubes, the view factor from the cartridge heater to the fuel tube was assumed unity.

The fuel tube, evaporator region, and insulator in the test configuration were modeled as a three node radiation network, approximated by the network of resistors shown in Figure 4 (Ozisik, 1985). In the initial analysis, the insulator was assumed to be "reradiating." This translates to a net radiation heat flux of zero in the insulated zone, implying that the zone emitted as much radiation as it received by radiation from the surrounding zones. In the computational model that was developed, this implies that all radiative energy emitted by the fuel tubes and evaporator that was "seen" by the insulator was subsequently re-emitted by the insulator back to the fuel tubes and evaporator. Details of the radiation network model are discussed in Bragg-Sitton (2004).

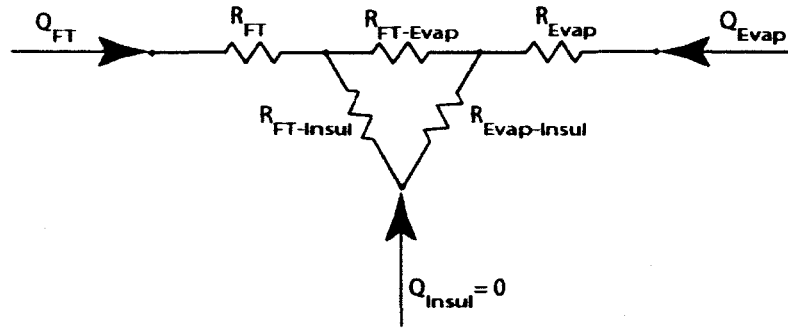


FIGURE 4. Three Node Radiation Network Applied for SAFE-100a Heat Pipe Module Analysis.

The amount of radiation each component sees is a function of the view factor. The view factor physically represents the fraction of the radiative energy leaving one surface that directly strikes the other surface of interest. The view factors ( $F$ ) between each component and the emittance of each component in the network are included in the equivalent resistances that appear in the network in Fig. 4.

The unsteady, one-dimensional diffusion equation with a heating source, radiation, and convection is given by:

$$C \frac{\partial T}{\partial t} = k \frac{\partial^2 T}{\partial x^2} + \dot{q} - G(T^4 - T_{\infty}^4) - hA(T - T_{\infty}) \quad (4)$$

Equation 4 can then be written in difference form about the cartridge heaters, fuel tubes, and evaporator (Bragg-Sitton, 2004). The original HPAPPX code only considered radial heat transfer, and the heat transfer rate from the evaporator to the first condenser node,  $Q_{(2)}$ , was determined by the minimum of the radiation, sonic and viscous limits. Addition of axial conduction through the sodium trapped in the annular gap in the heat pipe adds an additional term to the evaporator and condenser nodes:

$$Q_{axial} = kA \frac{\partial T}{\partial z} = \frac{T(j+1) - T(j)}{z(j+1) - z(j)} \quad (5)$$

Based on the current temperature of the node relative to the sodium melting temperature, the conductivity of solid or liquid sodium is selected. For the evaporator region, this represents an additional loss term (from node 1 to node 2); each of the condenser nodes sees heat addition due to axial conduction from the previous node, as well as heat loss to the subsequent node.

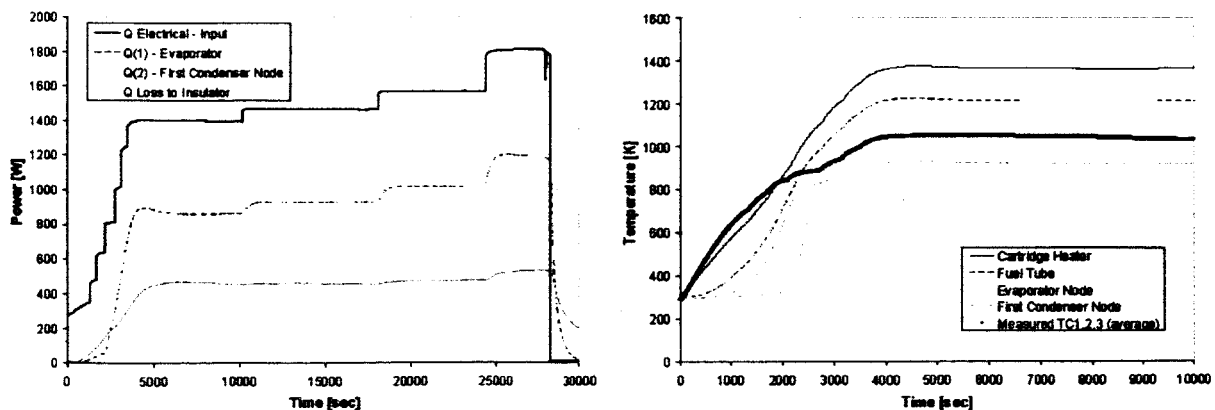
The Newton-Raphson method was employed to solve each of the energy balance equations at each time (Chapra and Canale, 1985). Because an initial guess is required, the Newton-Raphson method can find a local minimum as opposed to the global minimum that is sought. Hence, it is important that an appropriate initial guess be selected.

## RESULTS: COMPARISON OF COMPUTATIONAL AND EXPERIMENTAL ANALYSES

The accuracy of the computational model developed for SAFE-100a module operation was assessed by comparison to experimentally measured temperatures on the second start-up of SAFE-100a Module 12. Several changes in the geometry, material properties, and environmental boundary conditions were made to the original HPAPPX code to both make it applicable to the SAFE-100a geometry and testing conditions and to improve the details in the modeling. The modified HPAPPX code, also written in Fortran, will be referred to as SF100RADNtwk. Computational results for Module 12 are shown in Figures 5-6. The times at which each measurement was taken and the electrical power input to the heaters were required inputs to the computational model that were taken from the experimental data. The heat loss through the insulator was estimated by measured values reported by TC0 and TC16 at each measurement point. The electrical power input, measured power loss through the insulator, and calculated power into the evaporator and first condenser nodes are plotted in Figure 5a.

In Figure 5b, the average measured temperature is shown for thermocouples 1, 2, and 3 as compared to the predicted heater, fuel tube, evaporator, and condenser (node 2, evaporator exit/condenser entrance) temperatures. Because these thermocouples were located on the outside of each fuel tube (Fig. 2), these measured values would be expected to be lower than the calculated fuel tube temperature. However, one would expect the shape of the measured and calculated fuel tube temperatures to match somewhat better than what was obtained.

Because the trend in the calculated heater temperature matches the measured trend for the fuel tube temperature as a function of time, and the calculated fuel tube temperatures were lower than the average measured temperature on the outside surface of the fuel tube, it is likely that the modeled heat transfer from the heater to the fuel tube was insufficient. Recall that Eq. (3) assumed that heat was only transferred by radiation from the cartridge heater to the fuel tube. The model assumes that the heaters are centered in each fuel tube; in reality, each heater rests in the fuel tube (due to gravity), making contact with the fuel tube wall and providing an avenue for conduction that was not modeled see (Fig. 3c). All heat pipe start-up tests were performed in air for the SAFE-100a module, rather than in vacuum, such that a small amount of additional conduction may have been present between the heater and fuel tube, using air as a conduction medium. Although the total contribution from the conduction paths was expected to be small, experimental results suggest that conduction was the dominant means of heat transfer from the heater to the fuel tube (and, subsequently, to the evaporator) early in the start-up transient. This discrepancy in the model may have been sufficient to account for the modified shape in the fuel tube and evaporator temperature as a function of time. Additional error may have been introduced in the estimated heat loss through the insulator, or in the approximated convective losses around the fuel tube.



(a) Input Power and Calculated Output Power.

(b) Calculated Heater, Fuel Tubes, Evaporator, and First Condenser Node Temperatures.

FIGURE 5. SAFE-100a Module 12 Power and Temperatures.

The calculated and measured temperatures for the evaporator node and the first condenser node over the full test duration are shown in Figure 6a. Analysis of these results indicates that although the calculated evaporator and condenser temperatures were approximately correct during steady state, the temperature rise for each of these nodes was significantly delayed relative to the measured temperatures. Some fraction of this discrepancy may be attributed to the errors in the modeled heat transfer from the heaters to the fuel tubes, as discussed above. In addition, due to the relatively small contact area between the fuel tubes and the evaporator, it was assumed that conduction was negligible between these components. However, as shown in Fig. 3c, tricuspid material was used to bond the fuel tubes to the heat pipe, providing an avenue for conduction that was ignored in the model. As indicated in the illustration, the evaporator thermocouple was located on the outside of the evaporator, near the heater in the fuel tube. The physical location of this thermocouple also may have contributed to the higher measured temperature. Had the thermocouple been located between the bottom two fuel tubes, at a slightly greater distance from the cartridge heaters, it is likely that a lower temperature would have been measured. The combination of these effects (excluding conduction in the model and the physical location of the evaporator TC in the experiment) likely contributed to the delayed heating of the evaporator node (and, subsequently, the condenser nodes) in the calculated model versus experimental measurements.

Comparison of the computational results presented here using SF100RADNtwk for the SAFE-100a module to the earlier results obtained by Reid (2002) using the original HPAPPX for the SAFE-30 module demonstrates the importance of adding axial conduction to the heat balance model. Results presented by Reid (2002) predicted sharp increases in the condenser temperatures as the working fluid in these nodes was thawed. Axial conduction smooths the temperature rise over time. Although the calculated temperature rise for the first condenser node was slightly delayed relative to the measured data as a result of the modeling inaccuracies discussed above, the rate of the temperature rise (i.e. shape of  $T_{(2)}(t)$ ) was identical to the measured rate of temperature rise for node 2.

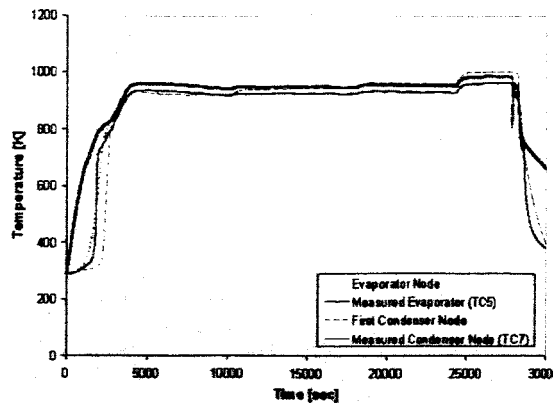
Figure 6b shows a comparison of the measured and calculated temperatures along the condenser for Module 12. Again, the temperature rise in each node was somewhat delayed relative to the measured values, but each maintains the appropriate rate of change and, with the exception of the final condenser node (node 9, TC14), each node in the condenser increases to the evaporator temperature at steady state. The final node (identified as  $T_{(9)}$ ) in the computational model failed to reach the evaporator temperature, reporting a value that was approximately 80 K lower than anticipated. This result may be due to the convection term along the insulator being too strong, or due to loss of heat by axial conduction to the stagnant sodium pool at the end of the condenser region. The final curve shown in Fig. 6 corresponds to the measured temperature of the heat pipe end cap. Because no sodium can flow into this region, the end cap temperature can only increase by conduction from the condenser, causing the end cap temperature to be significantly lower than the other condenser temperatures; the end cap temperature was not calculated in the computational model. The calculated temperature for node 9, which corresponds to the final condenser node adjacent to the end cap may be lower than anticipated due to modeling assumptions that reduce the effective length of the condenser region, such that in the model, node 9 appears to be a part of the stagnant sodium pool at the end of the heat pipe.

## CONCLUSIONS

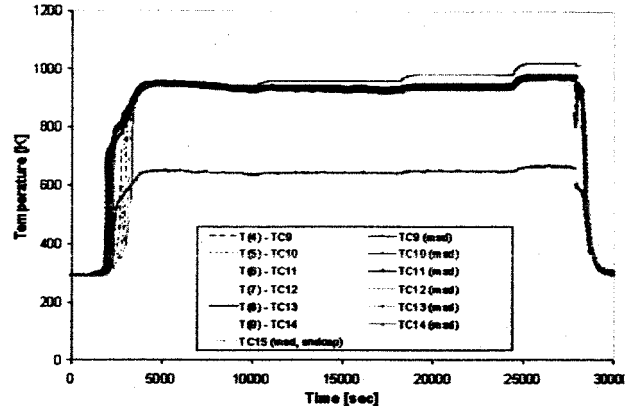
The modifications to the HPAPPX code for application to the SAFE-100a modules, which resulted in SF100RADNtwk, attempted a simple approach to modeling the transient operation of a SAFE-100a type heat pipe. Although the results that were obtained were reasonably accurate, several modifications could be applied to make the code more rigorous in its application.

First, it was noted that the heat transfer between the cartridge heaters and the fuel tubes was likely insufficient. Greater diligence should be applied to determine the magnitude of conduction from the heater to the fuel tube to better capture this behavior in the computational model. Other contributions to radial heat conduction should be assessed, including potential conduction between the fuel tubes and the heat pipe evaporator region.

Second, a more rigorous analysis of the radiation/conduction/convection heat transfer network between the fuel tubes, evaporator, and insulator should be completed. The current model incorporated heat loss through the insulator using measured boundary conditions; attempt should be made to dissociate the computational model from the experimental results as much as possible to avoid any potential biasing of the computational results.



(a) Evaporator and First Condenser Nodes.



(b) Condenser Node Temperatures.

FIGURE 6. Calculated and Measured Module 12 Temperatures.

Third, failure of the final condenser node to reach the evaporator temperature indicates a need to reassess the convection and axial conduction terms for the condenser nodes to determine the source of the error. It is likely that one or both of these terms is too high, causing the active region of the heat pipe to effectively be shortened.

Despite the small inaccuracies that result from simplifying assumptions, the SF100RADNtwk code provides a reasonable estimate of the heat pipe response under transient conditions. With the proper adjustments made to the boundary conditions, this code will be applied to heat pipe transient operation under vacuum conditions. In a vacuum environment, the simplifying assumptions made for the insulator heat loss and for the convection heat loss terms will be less significant, and it is anticipated that the computational results will better match the experimental data. Lifetime testing of the SAFE-100a modules and testing of the heat pipe modules in the electrically heated SAFE-100a core will commence in FY2004; all in-core and lifetime testing will be performed under vacuum conditions.

## NOMENCLATURE

$\epsilon$	= emittance of the heat pipe (condenser) surface (unitless)	$h_{fg}$	= latent heat of vaporization
$\gamma$	= specific heat ratio = $C_p/C_v = 5/3$ for monatomic gases	$k$	= conductivity (W/m <sup>2</sup> -K),
$\rho_o$	= stagnation density	$M$	= molecular weight of working fluid (g/mol)
$\sigma$	= Stefan - Boltzmann constant (W/m <sup>2</sup> -K <sup>4</sup> )	$p_o$	= stagnation pressure
$A$	= surface area (m <sup>2</sup> )	$\dot{Q}$	= energy transfer rate (W)
$A_{Cond}$	= outside surface area of the condenser (m <sup>2</sup> )	$R$	= effective resistance of the radiation network (m <sup>-2</sup> ),
$A_v$	= vapor flow area (m <sup>2</sup> )	$T_{Evap}$	= evaporator temperature (K), and
$C$	= specific heat capacity (J/K)	$T_\infty$	= temperature of the surrounding environment (K)
$G$	= conductance (W/K) = $\sigma/R$		
$h$	= convection coefficient (W/m-K)		

## ACKNOWLEDGMENTS

NASA's Project Prometheus, the Nuclear Systems Program, supported the work described within this paper as part of the program's technology development and evaluation activities. Any opinions expressed are those of the authors and do not necessarily reflect the views of Project Prometheus.

## REFERENCES

- Bragg-Sitton, S.M. (2004). *Analysis of Space Reactor System Components: Investigation Through Simulation and Non-Nuclear Testing*, Doctoral Dissertation, University of Michigan, Ann Arbor, MI.
- Cao, Y., and Faghri, A. (1992). "Closed-Form Analytical Solutions of High-Temperature Heat Pipe Startup and Frozen Startup Limitation." *Journal of Heat Transfer*, 114(4), 1028-1035.
- Chapra, S. C., and Canale, R. P. (1985). *Numerical Methods for Engineers*, McGraw-Hill, Inc., New York.
- Faghri, A. (1995). *Heat Pipe Science and Technology*, Taylor and Francis, Washington, D.C.
- Hall, M. L., and Doster, J. M. (1990). "A sensitivity study of the effects of evaporation/condensation accommodation coefficients on transient heat pipe modeling." *International Journal of Heat and Mass Transfer*, 33(3), 465-81
- Hall, M. L., M. A. Merrigan, and Reid, R. S. (1994). "Status Report on the THROHPUT Transient Heat Pipe Modeling Code." *Proc. 12th Symposium on Space Nuclear Power and Propulsion*, Albuquerque, NM, AIP Conf. Proc.
- Martin, J. J., and Salvail, P. (2004). "Sodium Heat Pipe Module Processing for the SAFE-100 Reactor Concept." *Space Technology and Applications International Forum 2004*, Albuquerque, NM, 148-155.
- Ozisik, M. N. (1985). *Heat Transfer: A Basic Approach*, McGraw-Hill Book Company, New York.
- Reid, R. S. (2002). "Heat Pipe Transient Response Approximation." *Space Technology and Applications International Forum - STAIF 2002*, Albuquerque, NM, 156-162.
- Reid, R. S. (2003). "Los Alamos Heat Pipe Primer." Institute for Space and Nuclear Power Studies, University of New Mexico, Short Course on Space Nuclear Power & Propulsion Systems Technology: Enabling Future Planetary Exploration.
- Reid, R. S., Sena, J. T., and Martinez, A. L. (2001). "Sodium Heat Pipe Module Test for the SAFE-30 Reactor Prototype." *Space Technology and Applications International Forum*, Albuquerque, NM, 869-874.
- Tournier, J. M. (2003). "Startup of High Temperature Heat Pipes from a Frozen State." Institute for Space and Nuclear Power Studies, University of New Mexico, Short Course on Space Nuclear Power & Propulsion Systems Technology: Enabling Future Planetary Exploration.
- Tournier, J. M., and El-Genk, M. S. (1995). "Transient analysis of the start-up of a water heat pipe from a frozen state." *Numerical Heat Transfer, Part A*, 28, 461-486.
- Tournier, J. M., and El-Genk, M. S. (1996). "Vapor flow model for analysis of liquid-metal heat pipe startup from a frozen state." *International Journal of Heat and Mass Transfer*, 39(18), 3767-3780.
- Tournier, J. M., and El-Genk, M. S. (2003). "Startup of a horizontal lithium-molybdenum heat pipe from a frozen state." *International Journal of Heat and Mass Transfer*, 46, 671-685.
- Tournier, J.-M., and El-Genk, M. S. (1995). "Transient Analysis of a Water Heat Pipe." *Proceedings of the ASME Winter Conference, Nov 28-Dec 3 1993*, New Orleans, LA, USA, 1-8.